*Science* **271**, 62 (1996).
17. P. A. Bunker, *Molecular Symmetry and Spectroscopy* (Academic Press, San Diego, CA, 1979).
18. W. Klopper and M. Schütz, *Chem. Phys. Lett.* **237**, 536 (1995).
19. M. Schütz, W. Klopper, H. Lüthi, S. Leutwyler, *J. Chem. Phys.* **103**, 6114 (1995).
20. M. Head-Gordon and T. Head-Gordon, personal communication.
21. J. K. Gregory and D. C. Clary, *J. Chem. Phys.* **102**, 7817 (1995).
22. A. H. Narten, W. E. Thiessen, L. Blum, *Science* **217**, 1033 (1982).
23. S. W. Peterson and H. A. Levy, *Acta Crystallogr.* **10**, 70 (1957).
24. Supported by NSF grants CHE-9123335 and CHE-9424482. The authors gratefully acknowlege M. Head-Gordon and T. Head-Gordon for helpful conversations and calculations and T. Robinson for valuable computer graphics assistance.

16 October 1995; accepted 31 October 1995

# Vibration-Rotation Tunneling Spectra of the Water Pentamer: Structure and Dynamics

K. Liu, M. G. Brown, J. D. Cruzan, R. J. Saykally

Far-infrared laser vibration-rotation tunneling spectroscopy was used to measure an intermolecular vibration (81.19198 wave numbers) of the isolated water ($D_2O$) pentamer. Rotational analysis supports the chiral, slightly puckered ring structure predicted by theory. The experimentally deduced interoxygen separations for the water clusters up to the pentamer showed exponential convergence toward the corresponding distance in bulk phase water.

The quasiplanar pentagonal structure formed from five doubly hydrogen-bonded water molecules appears to have a special role in chemical and biological systems. Whereas normal ice ($I_h$) consists of regular arrays of hexagons, molecular dynamics calculations (*1–3*) show the liquid (25°C) to be dominated by pentagons. The anomalous thermodynamic properties of liquid water have been rationalized in terms of fluctuations in the number of pentagons (*4*). Clathrate hydrate structures consist of water molecules organized in arrays of pentagons and hexagons around a central hydrophobe (*5*). A similar array of five-membered water rings occurs near the surfaces of proteins (*6*), DNA (*7*), and DNA-drug complexes (*8*). These latter examples reflect the ability of pentagons to form closed geometrical structures, which may be of general significance in the hydration of biological macromolecules.

The reason for the dominance of pentagons and hexagons in bulk water systems is that these are the smallest polygons that can produce O–O–O angles near the optimum (tetrahedral) value, which maximizes the hydrogen bond energy (*2*). There is consensus in the theoretical work as to the equilibrium structure of the water pentamer (*9–11*). The most stable form of the pentamer is a cyclic, slightly puckered ring (similar to the bent form of cyclopentane) in which each water molecule acts as both a single hydrogen bond donor and acceptor (Fig. 1).

Although numerous ab initio and semiempirical studies have addressed the water pentamer, it remained to be experimentally characterized. Vernon *et al.* (*12*) and Huisken *et al.* (*13*) observed the OH stretching bands by vibrational predissociation in a mass-selected molecular beam, and x-ray crystallography measurements established the basic structure of concatenated water pentagons in biopolymers (*6–8*). But these experiments lacked the precision required to establish definitively structure and properties. Here, we report the determination of the water pentamer structure. This work follows our recent studies of the water dimer (*14*), trimer (*15*), and tetramer (*16*) by far-infrared (far-IR) laser vibration-rotation tunneling (VRT) spectroscopy (*17*).

A total of 218 parallel ($\Delta K = 0$, where $K$ is the quantum number of the rotational angular momentum component along the molecular symmetry axis) transitions were fit to a symmetric top Hamiltonian (Table 1). The composite data set, together with a simulated stick spectrum produced by the fitted molecular parameters, is shown in Fig. 2. The observed spectrum was assigned unambiguously to an exact oblate symmetric top, as no asymmetry splitting had been resolved. No quantum tunneling features were evident within the spectral resolution (~2 MHz) of our experiment. An attempt to measure a first-order Stark effect was not successful for the pentamer. The signal in this experiment was determined to result from pure water clusters (*18*).

The size of the cluster responsible for the observed transitions was determined through the isotope mixture test described in our previous study of the water trimer (*15*). A measurement of the line intensity as a function of the $D_2O$ mole fraction in the sample yielded a cluster size of 5.14 ± 0.36 at the 95% confidence level. The pentamer transitions appear as featureless singlets, so the isotope mixture test was necessary to discriminate the pentamer signals from the absorptions of other clusters coexisting in the jet. The validity of this mixture test has also been established for VRT spectra of the water dimer, the pure and isotopically substituted trimer, and the tetramer (*16*).

Structural information is derived from an analysis of the observed spectral pattern. Because of the nature of a parallel transition for a symmetric top, the rotational constant about the unique symmetry axis cannot be determined by fitting the spectral line positions alone. Only the difference between ground and excited state values of this constant can be definitively established. Simulation of the intensity profile gave good agreement with the experimental profile only for a nearly planar ($A = B \sim 2C$) oblate top (see Fig. 2). The rotational constants thus obtained preclude assignment to a tetramer or hexamer.

On the basis of the measured rotational constants, the averaged interoxygen distances, $R$(O–O), estimated from a point-mass model for $(D_2O)_n$ [$n$ = 2, 3, 4 (*16*), and 5], can be fit to a reasonable exponential function (Fig. 3), as noted by Xantheas and Dunning in their ab initio work on small cyclic water clusters (*9*). The similar $R$(O–O) contraction (toward the bulk values) apparent in both experiment and theory clearly shows the "cooperative" effects in the hydrogen bonding network. The discrepancy between them is primarily a result of the difference between the equilibrium and vibrational averaged structures, which can be significant for such fluxional systems.

The quantum tunneling dynamics in the water pentamer are responsible for the ob-

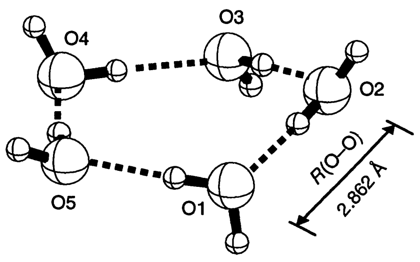

**Fig. 1.** Predicted equilibrium structure of the cyclic water pentamer. The coordinates used here are from the highest level available ab initio calculation, performed by Xantheas and Dunning (9). Other theoretical predictions give similar structural parameters. The dashed lines represent the hydrogen bonds. The calculated rotational constants *A*, *B*, and *C* for $(H_2O)_5$ structure are 1859, 1818, and 940 MHz, respectively. Because all five lateral distances are only slightly different, a typical *R*(O–O) is indicated here. The pentamer ring structure is puckered; the O1–O2–O3 plane bends about 20° from the O1–O3–O5 plane (O4 is approximately in this plane).

---

Department of Chemistry, University of California, Berkeley, CA 94720, USA.

served symmetric top structure and the absence of the expected tunneling features. These characteristics may be related to the rearrangements in the hydrogen bonding network that occur in liquid water. In the water trimer, two feasible tunneling pathways have been identified by experiment (*15*) and by Wales' theoretical treatment (*19*). First, the "flipping" of the free protons above and below the O–O–O plane causes the asymmetric equilibrium ring structure to average to a rigorously symmetric oblate top. The barrier to this motion is sufficiently low that the resulting large "tunneling" splitting (corresponding to the band origin) can actually be treated as a "pseudorotation," as demonstrated by Schütz *et al.* (*20*). Second, a higher barrier motion called donor tunneling—a motion analogous to that found in the water dimer (*21*)—gives rise to the observed quartet feature (smaller splitting).

The flipping and donor tunneling motions were also anticipated in the pentamer. Indeed, recent calculations by Wales (*22*) revealed two low-energy tunneling pathways entirely analogous to those found for the trimer. However, smaller splittings were expected for the predicted, slightly puckered pentamer. Such puckering requires the heavy oxygen atoms to move in concert with the light H or D atoms on completion of either pathway connecting the symmetrically equivalent forms, thereby reducing the tunneling frequency.

Invoking heavy atom motions in the pentamer inevitably impeded the motions in the already high barrier donor tunneling, which led to a smaller splitting than found for the trimer. Moreover, the stronger, many-body forces operating in the pentamer further hindered the motions of H or D with higher effective barriers. In $(D_2O)_3$, the observed small (~5 MHz) spacing within the quartet is the difference of the donor tunneling splittings between the upper and lower states. Therefore, we ascribed the featureless tunneling pattern found for the pentamer either to an unresolvable splitting or to nearly equal tunneling splittings in the ground and excited states; both are consistent with a process having a high effective barrier and increased tunneling mass. Measurement of the normal water pentamer, $(H_2O)_5$, would help resolve this matter, inasmuch as an ~60-fold increase of the donor tunneling splitting has been observed in $(H_2O)_3$ relative to $(D_2O)_3$. Again, Wales' calculations on pentamer tunneling dynamics (*22*) heighten interest in future studies of the normal isotope.

Finally, there is the nature of the observed intermolecular vibration to consider. Because of the large anharmonicity of the hydrogen bond, the theoretical harmonic intermolecular vibrational frequencies reported cannot be compared directly with experiment, which has already been shown in the smaller cluster studies. The small change in the ground and excited state rotational constants suggests that, as in the case of the water trimer, the observed intermolecular vibration at 81.1 $\mathrm{cm}^{-1}$ does not involve the hydrogen bond stretching. If it did, anharmonic effects would significantly alter the structural parameters during excitation. Moreover, the stiffness of the hydrogen bond stretch would require higher excitation energies [~150 $\mathrm{cm}^{-1}$ predicted for the water dimer (*23*)]. Accordingly, the low-frequency mode that we observed probably corresponds to torsional motions about the hydrogen

**Table 1.** Molecular constants for $(D_2O)_5$. The rovibrational transitions were assigned unambiguously to a parallel band. The Hamiltonian used in the fit was

$$[(A + B)J(J + 1)/2] + [(C - (A + B)/2)K^2] - [D_J(J(J + 1))^2] - [\mathrm{D}_{JK}J(J + 1)K^2]$$

where $J$ and $K$ are the quantum numbers of the total rotational angular momentum and its component along the molecular symmetry axis, respectively; $A$, $B$, and $C$ are the rotational constants; and $D_J$ and $D_{JK}$ are the distortion constants. The SDs are given in parentheses. Note that for a parallel transition, only the difference between $C''$ and $C'$ can be determined. The band origin $\nu_0$ occurs at 2434074.36 (55) MHz, and the root mean square error of the fit is 3.39 MHz.

| Parameter | Fitting results (MHz) |
|---|---|
| *Ground state* | |
| $A'' = B''$ | 1750.815 (76) |
| $C''$ | Arbitrarily fixed |
| $D_J''$ | 0.00159 (48) |
| $D_{JK}''$ | −0.0048 (15) |
| *Excited state* | |
| $A' = B'$ | 1751.163 (76) |
| $C' - C''$ | 7.6155 (86) |
| $D_J'$ | 0.00163 (48) |
| $D_{JK}'$ | −0.0048 (15) |

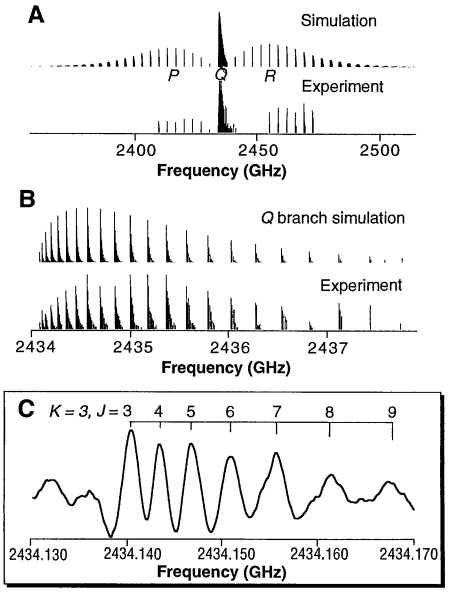

**Fig. 2.** Experimentally observed and simulated far-IR VRT spectra for the water pentamer. (**A**) Overall stick spectrum. Only the scanned spectral region is shown as the experimental spectrum. (**B**) Expansion of the $Q$ branch region. (**C**) The actual experimental spectrum of the $K = 3$ $Q$ branch subband. $J$ is the overall rotational quantum number, and $K$ is its component along the molecular symmetry axis. The simulated line positions were calculated with the fitted molecular parameters listed in Table 1. The intensity computation used Hönl-London and Boltzmann factors at a rotational temperature of ~5 K. The indeterminable $C$ constant was varied while maintaining the fitted value for $\Delta C$ ($C' - C''$). The observed spectral pattern can be reproduced only for $2C'' \sim A''$, a structural relation satisfied by a nearly planar oblate rotor. The discrepancy between them is a result of the long-term drift in the intensity measurements, which is most noticeable between the $P$, $Q$, and $R$ branches in (A), and less so within the $Q$ branch in (B). The Berkeley tunable far-IR spectrometer system has been described elsewhere (*25*).

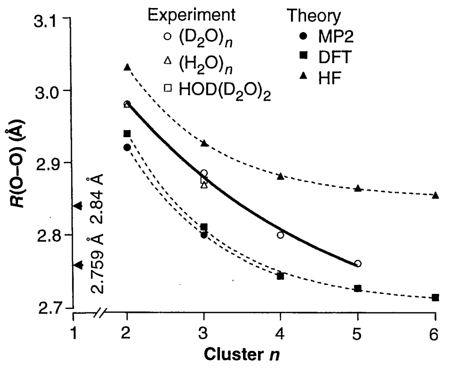

**Fig. 3.** Comparison of the O–O separations [$R$(O–O)] for various sizes of water clusters between experiment and theory. The experimental center-of-mass separations were determined from a simple point-mass model. For the cyclic clusters that are vibrationally averaged to become nearly planar oblate ($A = B$, unique condition) tops, only the averaged center-of-mass separation can be uniquely determined by adjusting an equilateral polygon (one variable model) with a point mass of the water molecule at each apex to reproduce the rotational constants. Because the center-of-mass separations are systematically larger than the $R$(O–O), the experimental values (open symbols) have been scaled (multiplied by 0.977) to reproduce the previously determined dimer $R$(O–O), 2.98 Å (*23*). Fitting the experimental $R$(O–O)s for $(D_2O)_n$ ($n$ = 2, 3, 4, and 5) resulted in the following expression: $R^{(n)}(\mathrm{O{-}O}) = 2.639 + 0.6981 \cdot \exp(-0.3566n)$. The ab initio predictions (*9*) (filled symbols) were obtained at different levels of theory: Hartree-Fock (HF), Møller-Plesset second-order perturbation theory (MP2), and density functional theory (DFT). Arrowheads indicate the experimental O–O distances in liquid water (2.84 Å at 4°C) (*26*) and in normal ice (2.759 Å at 223 K) (*27*).

bonds, such as flipping of the unbound D atoms, as in the water trimer (*15*), and perhaps is also associated with twisting and bending motions of the oxygen framework, as found in cyclopentane (*24*). Assigning the observed vibration to the flipping mode is consistent with (i) a parallel ($\Delta K = 0$) transition in which the dipole moment change associated with the out-of-plane vibration is parallel to the symmetry axis (perpendicular to the ring) and (ii) the fact that both the ground and the excited state structures are averaged to rigorously symmetric top forms by the flipping dynamics.

### REFERENCES AND NOTES

1. A. Rahman and F. H. Stillinger, *J. Am. Chem. Soc.* **95**, 7943 (1973).
2. R. J. Speedy, J. D. Madura, W. L. Jorgensen, *J. Phys. Chem.* **91**, 909 (1987).
3. G. Corongiu and E. Clementi, *J. Chem. Phys.* **98**, 2241 (1993).
4. R. J. Speedy, *J. Phys. Chem.* **88**, 3364 (1984).
5. J. H. van der Waals and P. C. Platteeuw, *Adv. Chem. Phys.* **2**, 1 (1959).
6. M. M. Teeter, *Proc. Natl. Acad. Sci. U.S.A.* **81**, 6014 (1984).
7. L. A. Lipscomb *et al.*, *Biochemistry* **33**, 3649 (1994).
8. S. Niedle, H. Berman, H. S. Shieh, *Nature* **288**, 129 (1980).
9. S. S. Xantheas and T. H. Dunning Jr., *J. Chem. Phys.* **99**, 8774 (1993); *ibid.* **98**, 8073 (1993); S. S. Xantheas, *ibid.* **102**, 4505 (1995).
10. R. Knochenmuss and S. Leutwyler, *ibid.* **96**, 5233 (1992).
11. K. S. Kim, M. Dupuis, G. C. Lie, E. Clementi, *Chem. Phys. Lett.* **131**, 451 (1986); P. L. M. Plummer and T. S. Chen, *J. Chem. Phys.* **86**, 7149 (1987); J. Pillardy, K. A. Olszewski, L. Piela, *J. Mol. Struct.* **270**, 277 (1992); W. B. Bosma, L. E. Fried, S. Mukamel, *J. Chem. Phys.* **98**, 4413 (1993); L. A. Burke, J. O. Jensen, J. L. Jensen, P. N. Krishnan, *Chem. Phys. Lett.* **206**, 293 (1993).
12. M. F. Vernon *et al.*, *J. Chem. Phys.* **77**, 47 (1982).
13. F. Huisken, M. Kaloudis, A. Kulcke, D. Voelkel, *Infrared Phys. Technol.* **36**, 171 (1995).
14. N. Pugliano, J. D. Cruzan, J. G. Loeser, R. J. Saykally, *J. Chem. Phys.* **98**, 6600 (1993).
15. N. Pugliano and R. J. Saykally, *Science* **257**, 1937 (1992); K. Liu *et al.*, *J. Am. Chem. Soc.* **116**, 3507 (1994); K. Liu *et al.*, *Faraday Discuss. Chem. Soc.* **97**, 35 (1994).
16. J. D. Cruzan *et al.*, *Science* **271**, 59 (1996).
17. R. J. Saykally and G. A. Blake, *ibid.* **259**, 1570 (1993).
18. To investigate the possibility of having buffer gas atoms in the observed cluster signal, we used several different noble gases (Ar, He, and a mixture of 70% Ne with He) as the supersonic expansion carrier gas. In all cases, identical absorption signals were observed without any frequency shift; a rare gas-containing cluster with the same water chromophore would have exhibited a significant frequency shift on substitution of the rare gas component.
19. D. J. Wales, *J. Am. Chem. Soc.* **115**, 11180 (1993).
20. M. Schütz, T. Bürgi, S. Leutwyler, H. B. Bürgi, *J. Chem. Phys.* **99**, 5228 (1993).
21. G. T. Fraser, *Int. Rev. Phys. Chem.* **10**, 189 (1991).
22. D. J. Wales, unpublished data.
23. T. R. Dyke, K. M. Mack, J. S. Muenter, *J. Chem. Phys.* **66**, 498 (1977).
24. J. E. Kilpatrick, K. S. Pitzer, R. Spitzer, *ibid.* **69**, 2483 (1947).
25. G. A. Blake *et al.*, *Rev. Sci. Instrum.* **62**, 1701 (1991). Briefly, tunable far-IR light is generated by mixing an optically pumped far-IR laser with continuously tunable microwave (mw) radiation in a Schottky barrier diode. The resulting tunable side bands ($\nu_{\text{far-IR}} \pm \nu_{\text{mw}}$) are directed into a vacuum chamber where they are multipassed 22 times nearly orthogonal to a pulsed planar supersonic jet containing clusters of interest. The direct absorption signal is detected by a liquid He–cooled stressed Ga:Ge photoconductor. Jet-cooled water clusters were produced by bubbling Ar through room-temperature water and expanding the saturated gas through a pulsed 101.6 mm by 0.100 mm slit nozzle.
26. A. H. Narten and H. A. Levy, in *Water: A Comprehensive Treatise*, F. Franks, Ed. (Plenum, New York, 1972), vol. 1, pp. 311–332.
27. W. F. Kuhs and M. S. Lehmann, *J. Phys. Chem.* **87**, 4312 (1983).

28. Supported by the Experimental Physical Chemistry Program of the National Science Foundation (CHE-9424482). We thank J. G. Loeser and M. J. Elrod for enlightening discussions.

28 July 1995; accepted 25 October 1995

# Role of Mutant CFTR in Hypersusceptibility of Cystic Fibrosis Patients to Lung Infections

Gerald B. Pier,* Martha Grout, Tanweer S. Zaidi, John C. Olsen, Larry G. Johnson, James R. Yankaskas, Joanna B. Goldberg

Cystic fibrosis (CF) patients are hypersusceptible to chronic *Pseudomonas aeruginosa* lung infections. Cultured human airway epithelial cells expressing the ΔF508 allele of the cystic fibrosis transmembrane conductance regulator (CFTR) were defective in uptake of *P. aeruginosa* compared with cells expressing the wild-type allele. *Pseudomonas aeruginosa* lipopolysaccharide (LPS)–core oligosaccharide was identified as the bacterial ligand for epithelial cell ingestion; exogenous oligosaccharide inhibited bacterial ingestion in a neonatal mouse model, resulting in increased amounts of bacteria in the lungs. CFTR may contribute to a host-defense mechanism that is important for clearance of *P. aeruginosa* from the respiratory tract.

Among the most serious manifestations of CF are chronic pulmonary infections with the bacterium *P. aeruginosa*. The basis for hypersusceptibility of CF patients to this bacterium is not well understood, and the role of mutant CFTR, if any, is not clear. Binding and internalization of respiratory pathogens by epithelial cells followed by desquamation could be an important mechanism for clearing bacteria from the lung. This mechanism has been shown to be important in protecting against bladder infections (*1*).

To investigate whether the most common and severe CFTR mutation (ΔF508) affected uptake of *P. aeruginosa*, we performed bacterial invasion assays (*2*) with four cell lines: CFT1, an airway epithelial cell line derived from a CF patient homozygous for ΔF508 CFTR and that is transformed with human papilloma virus 18 E6/E7; CFT1-ΔF508, which expresses a third copy of ΔF508 CFTR introduced by a retrovirus; CFT1-LC3, which expresses a control gene (β-galactosidase) introduced by the same retrovirus; and CFT1-LCFSN, which expresses a functional wild-type human CFTR gene (*3*). We tested a standard laboratory strain of *P. aeruginosa*, designated PAO1, and two nonmucoid, LPS-smooth clinical isolates from CF patients (*4*). Compared with CFT1-LCFSN cells, the three lines expressing ΔF508 CFTR internalized significantly fewer bacterial cells (Fig. 1A). The ΔF508 mutation causes inefficient processing of CFTR, a defect that is partially corrected if the cells are grown at 26°C (*5*). When epithelial cells were cultured for 72 hours at 26°C there were no longer significant differences in uptake of the *P. aeruginosa* strains by the cells expressing wild-type or mutant CFTR (Fig. 1B). Because the overall uptake of bacteria at 26°C was low, we performed additional experiments with cells grown for 72 hours at 26°C in which the invasion assay was performed at 37°C for 3 hours, conditions under which surface expression of mutant ΔF508 CFTR is maintained (*5*). No significant difference in bacterial cell uptake was measured (Fig. 1C), and overall amounts of internalization approached those of the CFT1-LCFSN cells at 37°C. Returning cells expressing ΔF508 CFTR to 37°C for 24 hours after growth for 72 hours at 26°C removes CFTR from the cell surface (*5*); under these conditions internalization of the bacterial strains was essentially identical to that shown in Fig. 1A (*6*). These data indicate that internalization of *P. aeruginosa* by airway epithelial cells correlated with membrane expression of CFTR.

The effect of ΔF508 CFTR on ingestion appeared to be specific for *P. aeruginosa*; other bacterial pathogens tested (*7*) were internalized equally well by cells expressing mutant ΔF508 or wild-type

---

G. B. Pier, M. Grout, T. S. Zaidi, J. B. Goldberg, Channing Laboratory and Department of Medicine, Brigham and Women's Hospital, Harvard Medical School, 180 Longwood Avenue, Boston, MA 02115-5899, USA.
J. C. Olsen, L. G. Johnson, J. R. Yankaskas, Department of Medicine, Division of Pulmonary Diseases, University of North Carolina, Chapel Hill, NC 27599-7020, USA.

*To whom correspondence should be addressed.